Geomechanics and Engineering, *Vol. 8, No. 6 (2015) 757-767*
DOI: http://dx.doi.org/10.12989/gae.2015.8.6.757

Mechanical and fracture behavior of rock mass with parallel concentrated joints with different dip angle and number based on *PFC* simulation

Weihua Zhao [*], Runqiu Huang [b] and Ming Yan [c]

State Key Laboratory of Geological Hazard Prevention and Geological Environment Protection, Chengdu University of Technology, Chengdu, Sichuan 610059, China

(*Received September 15, 2014, Revised January 14, 2015, Accepted January 16, 2015*)

Abstract. Rock mass is an important engineering material. In hydropower engineering, rock mass of bank slope controlled the stability of an arch dam. However, mechanical characteristics of the rock mass are not only affected by lithology, but also joints. On the basis of field geological survey, this paper built rock mass material containing parallel concentrated joints with different dip angle, different number under different stress conditions by *PFC* (Particle Flow Code) numerical simulation. Next, we analyzed mechanical property and fracture features of this rock mass. The following achievements have been obtained through this research. (1) When dip angle of joints is 15° and 30°, with the increase of joints number, peak strength of rock mass has not changed much. But when dip angle increase to 45°, especially increase to 60° and 75°, peak strength of rock mass decreased obviously with the increase of joints number. (2) With the increase of confining stress, peak strengths of all rock mass have different degree of improvement, especially the rock mass with dip angle of 75°. (3) Under the condition of no confining stress, dip angle of joints is low and joint number is small, existence of joints has little influence on fracture mode of rock mass, but when joints number increase to 5, tensile deformation firstly happened at joints zone and further resulted in tension fracture of the whole rock mass. When dip angle of joints increases to 45°, fracture presented as shear along joints, and with increase of joints number, strength of rock mass is weakened caused by shear-tension fracture zone along joints. When dip angle of joints increases to 60° and 75°, deformation and fracture model presented as tension fracture zone along concentrated joints. (4) Influence of increase of confining stress on fracture modes is to weaken joints' control function and to reduce the width of fracture zone. Furthermore, increase of confining stress translated deformation mode from tension to shear.

Keywords: mechanical behavior and fracture characteristics; parallel concentrated joints, different dip angle of joints; different number of joints; *PFC* simulation

1. Introduction

It is well known that the properties of a rock mass depend not only on the properties of the intact rock and the joints individually, but also how they interact. (Pal *et al*. 2012). Structural Cybernetics hold that deformation and failure caused by joints plays a more important role in the whole rock mass engineering (Sun *et al*. 2014, Wang *et al*. 2014). So far, about mechanical

∗Corresponding author, Ph.D., E-mail: weihuageo@gmail.com

http://www.techno-press.org/?journal=gae&subpage=7 ISSN: 2005-307X (Print), 2092-6219 (Online)

properties of rock mass, many researchers have conducted extensive physical experiments, numerical simulations and mechanics theory researches, such as rock mass with different dip angle (Chen *et al*. 2013), different roughness feature (Gehle and Kutter 2003, Prudencio and Jan 2007, Song *et al*. 2013), different number (Sun *et al*. 2014) and different connectivity (Hoek and Bieniawski 1965, Pu and Cao 2012, Zhou *et al*. 2014) and under different stress condition (Reik and Zacas 1978, Cording and Jamil 1997, Yang *et al*. 2009). These studies illustrate impact of joints on rock strength and deformation and have made abundant achievements. But study on mechanical behavior, deformation and fracture characteristics of rock mass containing parallel concentrated joints is still relatively less. During field geological investigation, we found that concentrated joints are well developed in the slope rock mass and present some deformation phenomena (Fig. 1). In order to study mechanical behavior and facture characteristics of rock mass with parallel concentrated joints, we adopted discrete element method *PFC* (Particle Flow Code) (Itasca Consulting Group 2008) to conduct a series of numerical simulation of jointed rock mass composed by a large number of particle materials and contacts between particles. PFC is a DEM method introduced by Cundasll (1971) to analyse rock-mechanics problems. The most common method for simulating joints in PFC is the bond removal method that removing bonds between particles along the joint track (Cundasll 2000) and this method was widely used to study behaviour of rock joints (Kusumi *et al*. 2005, Jing and Stephansson 2007, Park and Song 2009, 2013).

2. Experiment design and test parameters

In *PFC*, the simulate model is composed by particles and contacts between particles. In order to make mechanical properties of simulated model coincide with actual rock mass, *Fishtank* in *PFC* is used and biaxial test is performed. The top and bottom walls act as loading platens and the velocities of the side walls are controlled by a servo-mechanism to maintain a constant confining stress (Itasca Consulting Group 2008). Joints are generated by the command *JSET* (Fig. 2), which generated either an individual joint plane or a set of joint planes. Joint-plane contacts can be assigned a contact model and properties that are different from those assigned to contacts not falling on the plane (Itasca Consulting Group 2008).

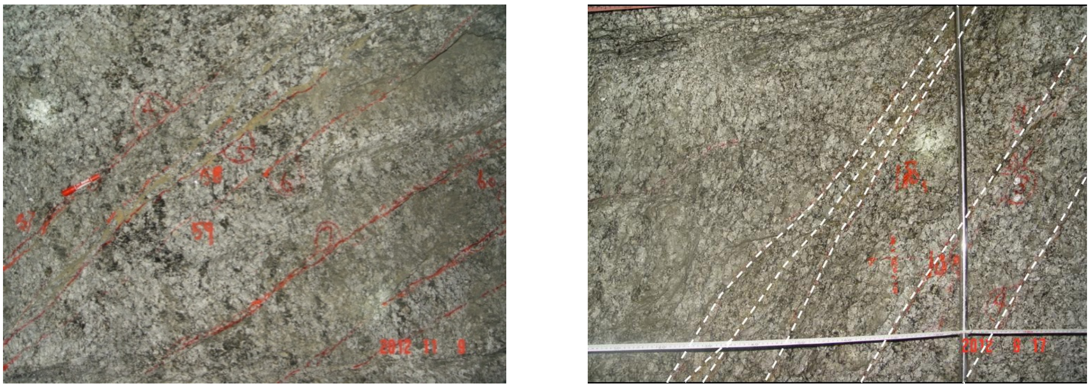

(a) (b)

Fig. 1 Concentrated joints zone in field (Lithology is Granite)

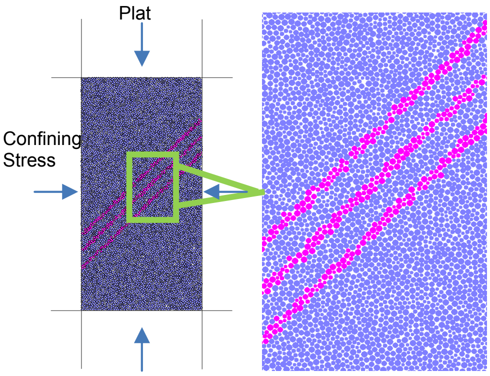

Fig. 2 Numerical model of jointed rock mass sample

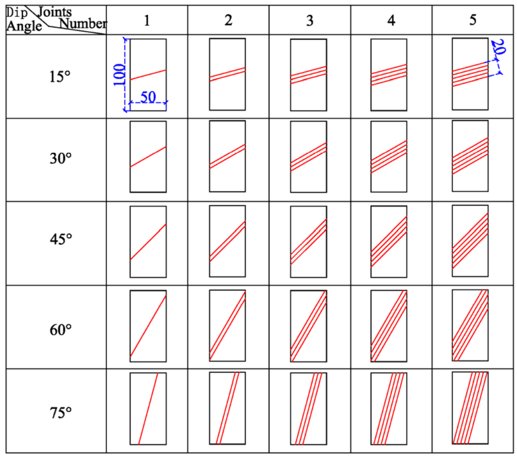

Fig. 3 Comparison test design of parallel jointed rock mass (unit: 10^{-3}m)

In this paper, dip angle, joints number are major concerned (spacing are major concerned in another paper) as influence factors for rock mass mechanical properties. Therefore, we designed the following schemes (Fig. 3): (1) dip angles of joints are designed from 15° to 75°; (2) joints number increased from 1 to 5; (3) confining stress set as 0 and 10 MPa the two stages.

Sample size of model this paper generated is 50 mm × 100 mm. Radius of particles follows Gaussian distribution that $R_{\min}$ = 0.30 mm, $R_{\max}$ = 1.66$R_{\min}$ = 0.498 mm. 8397 particles are generated and the porosity is 0.164. The micro-parameters of numerical sample are shown in Table 1. The micro-scale properties of the bonded particle model are commonly calibrated against the uniaxial compressive strength, elastic modulus and Poisson's ratio (Itasca Consulting Group 2008). Uniaxial compression tests were carried out and comparison between the results of numerical and experimental are listed in Table 2. The Table 2 showed that the results of simulation and physical experiments are in good agreement.

Table 1 Micro-parameters of numerical sample

Particles				Parallel contact						
Density ρ (kg/m^3)	Young's modulus E_c (GPa)	Normal/shear strength k_n/k_s	Friction coefficient μ	Radius factor $\bar{\lambda}$	Young's modulus $\bar{E}_c$ (GPa)	Normal/shear stiffness $\bar{k}_n/\bar{k}_s$	Normal strength $\bar{\sigma}_c$ (MPa)		Shear strength $\bar{\tau}_c$ (MPa)	
							Mean	Std	Mean	Std
2827	20	1.0	0.60	1.0	20	1.0	60	10	60	10

Table 2 Comparative results of physical and numerical uniaxial compression tests of intact rock

Test model	Unit weight γ (kg/m^3)	Uniaxial compressive strength (MPa)	Elastic modulus (GPa)	Poisson's ratio
Physical test	20~26.6	70~151	20~35	0.15~0.29
Numerical test	23.6	80	31.8	0.18

3. Results analysis

3.1 Stress-strain characteristics of rock mass with joints

Fig. 4 showed the stress-strain curves of rock mass with different number and different dip angles of joints under confining 0 (*A*) and 10 MPa (*B*) respectively. From the Fig. 4, the following results are obtained.

(1) Under the same confining stress, for the same dip angle, when dip angle of joints is 15° and 30°, stress-strain curves only have small difference. But when dip angle increases to 45°, 60° and 75°, difference between stress-stain curves become more and more obvious. This illustrated that low-angle dip joints have small influence on rock mass. But with the increase of dip angle and joints number, strength of rock mass decreased rapidly.

(2) With the increase of confining stress, strength of rock mass all have different degrees of increase. The most obvious change is 75° dip angle. When confining stress is 0, the lowest peak strength is 20 MPa (5 joints) and the highest peak strength is 47.8 MPa. When confining stress is 10MPa, the lowest peak strength is 58.9 MPa and the highest peak strength is 75.6 MPa.

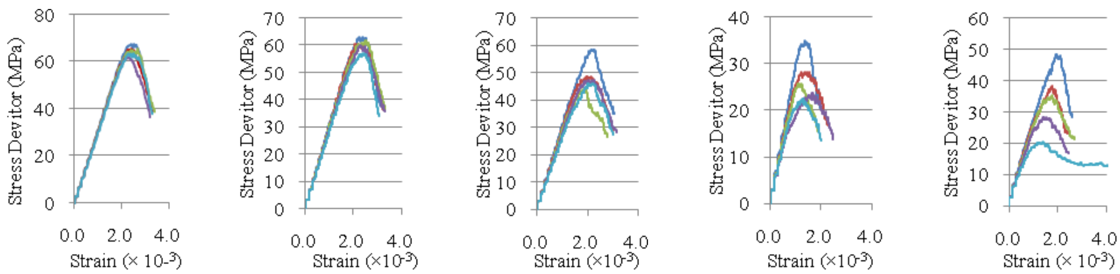

(a) Dip angle = 15° (b) Dip angle = 30° (c) Dip angle = 45° (d) Dip angle = 60° (e) Dip angle = 75°

(A) Stress-strain curves of rock mass under confining stress = 0 MPa

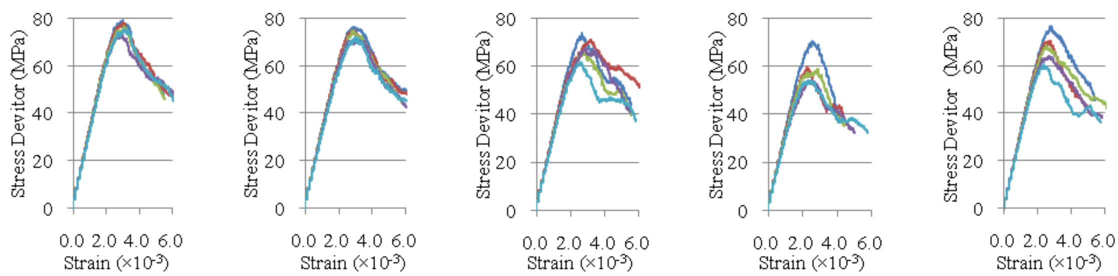

(a) Dip angle = 15° (b) Dip angle = 30° (c) Dip angle = 45° (d) Dip angle = 60° (e) Dip angle = 75°

(B) Stress-strain curves of rock mass under confining stress = 10 MPa

Fig. 4 Stress-strain curves of jointed rock mass with different number and dip angle under different confining stress

Deformation and failure type could be judged by stress-strain curve shapes. When confining stress is 0 and dip angle of joints are 15°, 30° and 45°, strain corresponding to peak strength is larger than 2%. When dip angle of joints are 60° and 75°, strain corresponding to peak strength is 1%~2%. Post-peak stress-strain curves fall quickly. These illustrated that deformation types of rock mass are mainly shear and tension. When the confining stress increase to 10 MPa, strain corresponding to peak strength is about 3%, and stress-strain curves fall slowly. At this time, deformation types of rock mass are mainly shear and shear flow.

3.2 Fracture characteristics of rock mass with joints

Tables 3 and 4 showed the fracture characteristics of rock mass with different number, different dip angles of joints under different confining stress when post-peak strength is 60% of peak strength. Seen from Tables 3 and 4, fracture characteristics presented as follow:

(1) When confining stress is 0 MPa, axial strain of rock mass is just 2%~3%. And when confing stress is 10 MPa, axial strain of rock mass is about 6%. Compared with under 0 MPa, the rock mass developed larger displacement under 10 MPa confining stress.

(2) Intact rock mass developed conjugate shear fracture both under 0 and 10 MPa confining stress.

(3) When confining stress is 0 MPa, fractures of rock mass with different number and different dip angle joints mainly showed as follow:

   (i) For rock mass with one 15° joint, fracture characteristic is similar to intact rock mass. But with the increase of joints number, influence of joints grows. Displacement firstly presents reverse movement at two ends of joints. Then tension developed in the middle of the whole mass.
   (ii) When dip angle of joints is 30°, for one joint, location and mode of main fracture changed a little. We can see displacement and shear along joint and main fracture is perpendicular to the joint. With increase of joints number, shear and tension phenomena become more and more obvious.
   (iii) When dip angle of joints is 45°, for one joint, the rock mass sheared along the joint.

Table 3 Deformation and fracture features of rock mass with different dip angle, different number joints under 0 MPa confining stress (post-peak strength = 60% peak strength)

Dip angle	One joint	Two joints	Three joints	Four joints	Five joints	Intact rock mass
15°	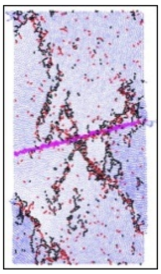	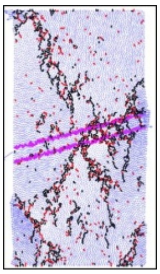	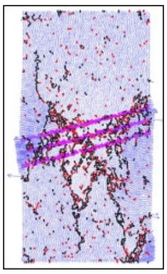	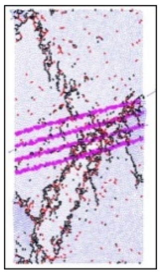	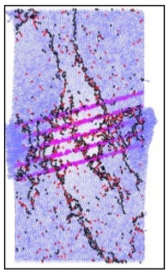	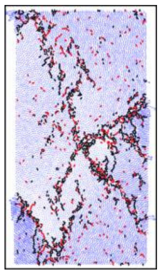

Table 3 Continued

Dip angle	One joint	Two joints	Three joints	Four joints	Five joints	Intact rock mass
30°	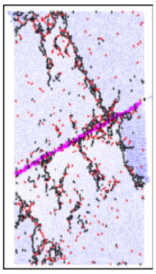	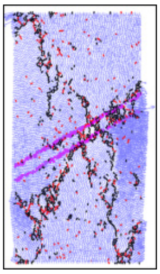	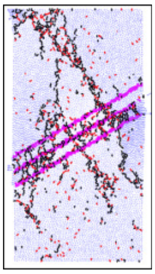	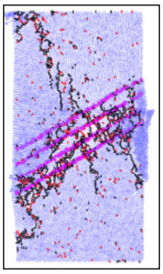	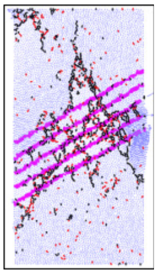	Legend 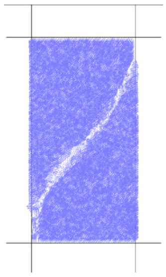
45°	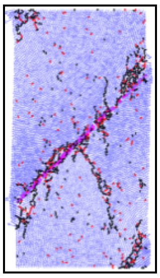	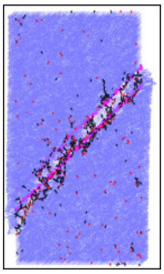	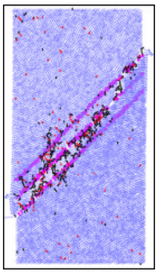	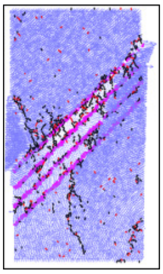	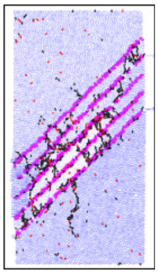	Displacement vector 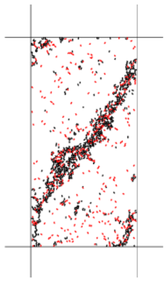
60°	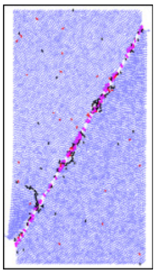	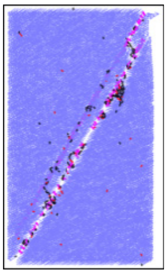	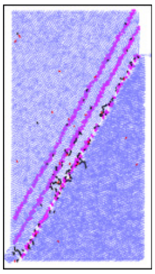	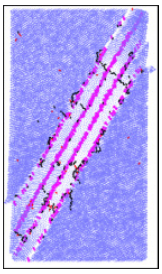	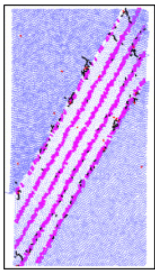	Fracture composed by micro-crack 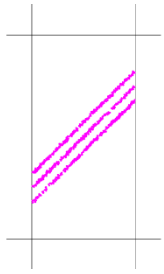
75°	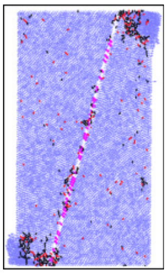	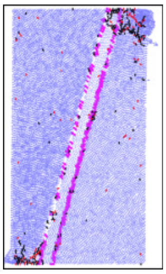	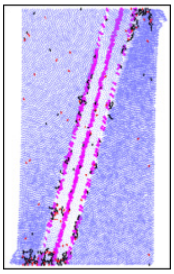	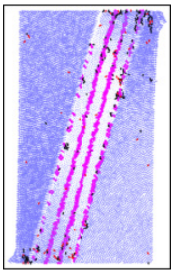	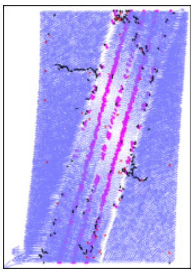	Joins

with increase of joints number, the rock mass sheared along the joints zone shaped as stair that the fracture is a shear zone. So joints controlled shear deformation and fracture of rock mass.

(iv) When dip angle of joints is 60° and 75°, the deformation and fracture mainly shown as tension along joints. With the increase of joints number, tension firstly occurred at outer joint, and then gradually tension inward. Finally, tensile fracture zone are developed controlled by joints.

(4) When confining stress is 10 MPa, fractures of rock mass with different number and different dip angle joints mainly showed as follow:

(i) When dip angle of joints is 15°, with increase of joints, deformation and fracture mode has not changed much. And the fracture characteristic is similar to intact rock mass. This illustrated that increase of confining stress weakened joints effect.

(ii) When dip angle of joints is 30°, for one joint, rock mass developed two parallel fracture. With increase of joints number, main fracture presented protion (right side) shear along joints and portion (left side) develped in matrix. And there is a fracture in the above of the main fracture.

(iii) When dip anlge of joints is 45°, fracture is still mainly along joints. But the total width of shear zone is obviously decreased.

(iv) For steep dip anlge of 60° and 75°, when confining stress is 0, displacement vectors mainly toward lateral side and have large angle with joints dip. But when confining stress is 10 MPa, angle between displacement vectors and joints become smaller. This illustrated that rock mass no longer showed pure tensile deformation, but showed shear-tensile deformation containing a certain shearing action.

3.3 Comparison analysis of simulated results and field phenomena

During field investigation, we found some typical deformation phenomena of rock mass with concentrated joints with different dip angle and number showed from Figs. 5 to 9. This paper compared the field phenomena and numerical simulations results. From these figures, we could found some results as follow:

(1) Fig. 5 showed two jointed rock mass with dip angle 15°. We can see the shear deformation along the joints, and quartz vein was dislocated by the shear action. In the first figure, tension cracks are developed between gentle dip joints. The two figures illustrated that shear deformation played a vital role.

(2) Fig. 6 showed shear action along joints. However, in the shearing process, these gentle dip joints are disconnected, and the shearing action is disrupted. The shear energy of the upper joint then results in tensile fractures between the upper and lower parallel joints. The shear joints and tensile fractures finally combine to form a diamond-shaped shear and tensile block. In the diamond-shaped block, tensile cleavages are well developed. The two figures demonstrated interaction effects of joints is more obvious compared to joints with dip angle 15°. More tension cracks between joints also can be seen in figures in row 30° in Table 3.

(3) In Fig. 7, we could see shear dilatancy along single joint. And in the second figure, concentrated joints are developed. All joints are filled with yellow mud. Some joints joined together at bottom. The phenomena are similar to the figures in row 45° in Table 3.

(4) With steep dip angles of 55° and 72°, tension deformation play a dominant role in Fig. 8 and Fig. 9. Especially in Fig. 9, all joints of the whole belt are tensioned and filled

Table 4 Deformation and fracture features of rock mass with different dip angle, different number joints under 10 MPa confining stress (post-peak strength = 60% peak strength)

Dip angle	One joint	Two joints	Three joints	Four joints	Five joints	Intact rock mass
15°	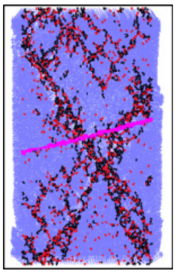	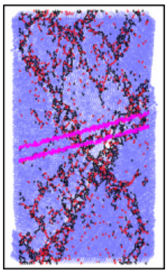	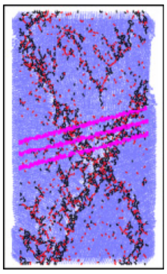	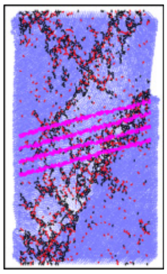	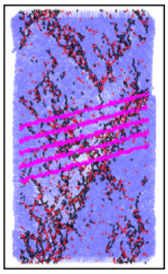	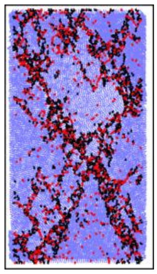
30°	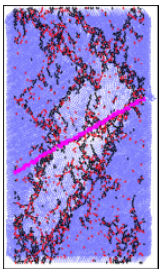	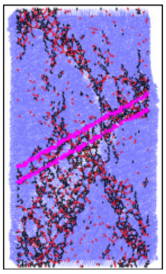	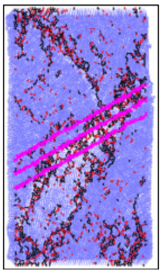	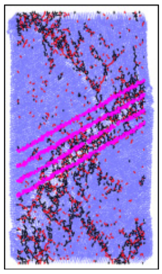	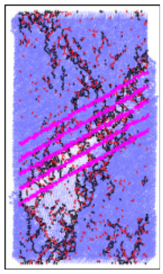	Legend 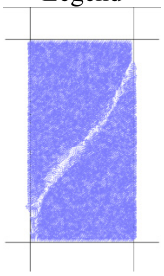 Displacement vector
45°	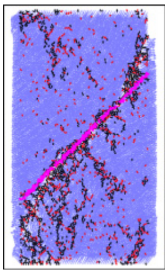	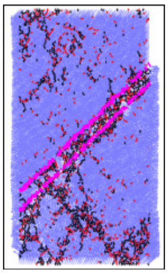	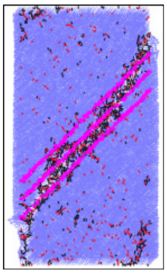	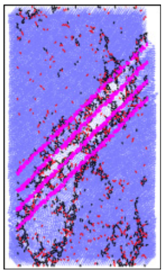	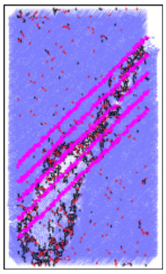	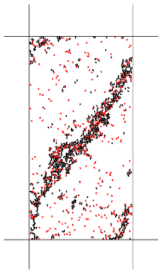 Fracture composed by micro-crack
60°	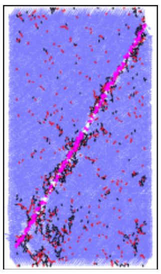	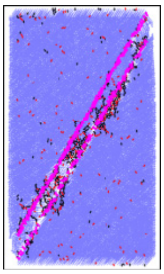	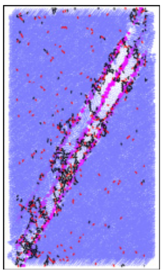	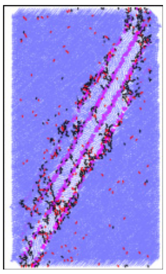	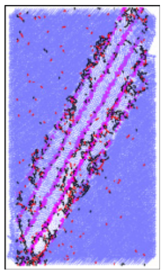	
75°	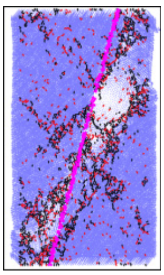	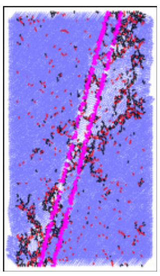	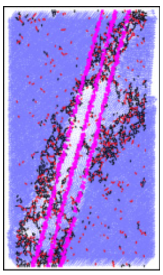	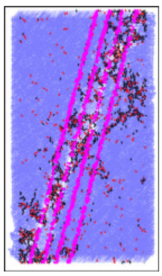	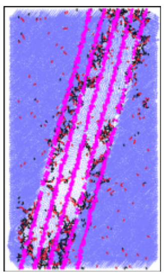	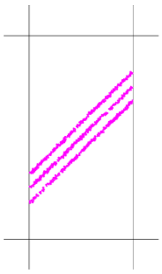 Joins

lots of yellow mud. The fracture opening of the two joints at sides is bigger than the middle joints. These phenomena also verified the figures in row 75° in Tables 3 and 4.

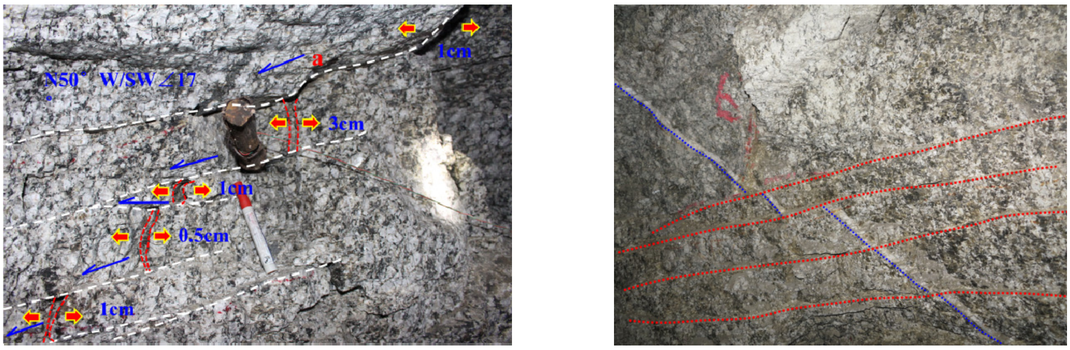

(a) (b)

Fig. 5 Typical phenomena of rock mass with joints of dip angle 15°

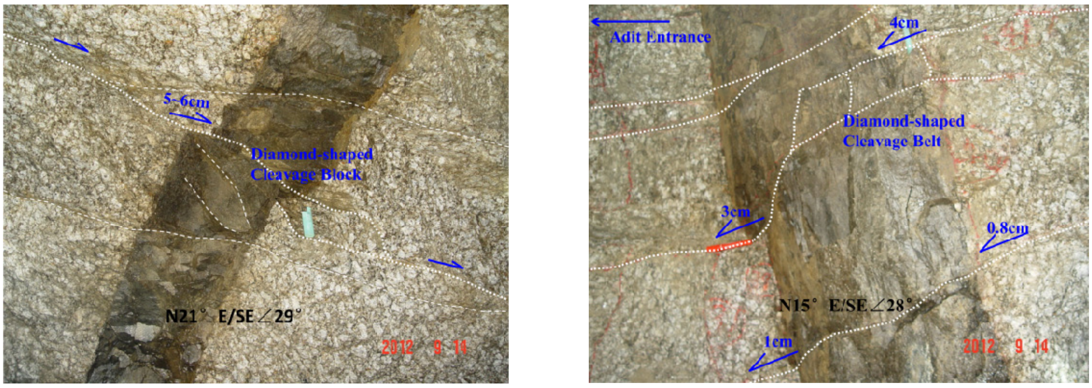

(a) (b)

Fig. 6 Typical phenomena of rock mass with joints of dip angle 30°

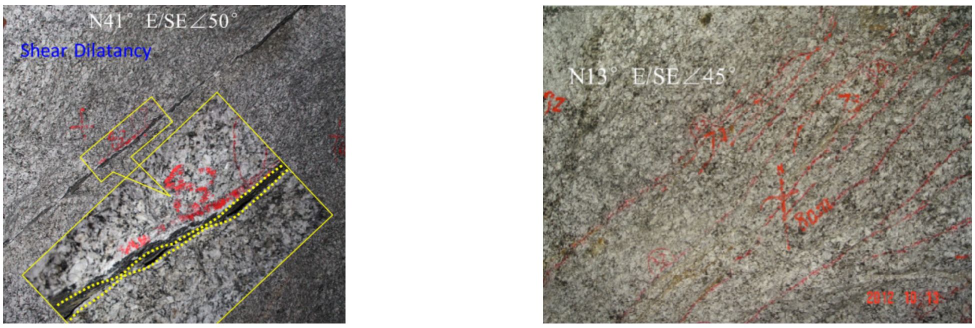

(a) (b)

Fig. 7 Typical phenomena of rock mass with joints of dip angle 45°

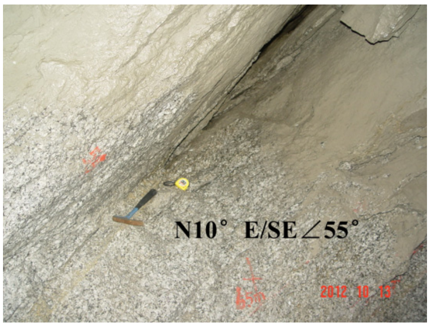

Fig. 8 Typical phenomena of rock mass with joints of dip angle 55°

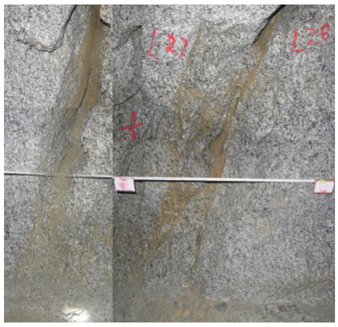

Fig. 9 Typical phenomena of rock mass with joints of dip angle 72°

4. Conclusions

On the basis of field geological survey, this paper built rock mass material containing parallel concentrated joints with different dip angle, different number under different stress condition by *PFC* (Particle Flow Code) numerical simulation. We analyzed mechanical property and fracture features of this rock mass. The following achievements have been obtained through this research.

- When dip angle of joints is 15° and 30°, with the increase of joints number, peak strength of rock mass has not changed much. But when dip angle increases to 45°, especially increases to 60° and 75°, peak strength of rock mass decreased obviously with the increase of joints number.
- With the increase of confining stress, peak strengths of all rock mass have different degree of improvement, especially the rock mass with dip angle of 75°.
- Under the condition of the 0 confining stress, dip angle of joints is low and joint number is small, existence of joints has little influence on fracture mode of rock mass, but when joints number increase to 5, tensile deformation firstly happened at joints zone and further resulted in tension fracture of the whole rock mass. When dip angle of joints increase to 45°, fracture presented as shear along joints, and with increase of joints number, strength of rock mass is weakened caused by shear-tension fracture zone along joints. When dip angle of joints increase to 60° and 75°, deformation and fracture model presented as tension fracture zone along concentrated joints.
- Influence of increase of confining stress on fracture mode is to weaken joints' control function and to reduce the width of fracture zone. Furthermore, increase of confining stress translated deformation mode from tension to shear.
- For rock mass with concentrated joints, mechanism and deformation characteristics are still influenced by other factors, such as spacing, total width, uneven spacing and filling of joints. This is still needs further studies and physical experiments still need more research.

Acknowledgments

This study is financially supported by Key Project of National Natural Science Foundation of China (Grant No. 41130745). We are also grateful to the reviewers for their useful comments and suggestions.

References

Chen, X., Liao, Z.H. and Peng, X. (2013), "Cracking process of rock mass models under uniaxial compression", *J. Cent. South Univ.*, **20**, 1661-1678. DOI: 10.1007/s11771-013-1660-2

Cording, E. and Jamil, M. (1997), "Slide geometries on rock slopes and walls", *Fourth South American Congress on Rock Mechanics*, Santiago, [s.n.], pp. 199-221.

Cundall, P.A. (1971), "A computer model for simulating progressive large scale movements in blocky rock systems", *Proceedings of the Symposium of the International Society of Rock Mechanics*, Nancy, France, Volume1, Paper No.11-8.

Cundall, P.A. (2000), "Numerical experiments on rough joints in shear using a bonded particle model", *Aspects of Tectonic Faulting*; Springer, Berlin, Germany, pp. 1-9. DOI: 10.1007/978-3-642-59617-9_1

Gehle, C. and Kutter, H.K. (2003), "Breakage and shear behavior of intermittent rock joints", *Int. J. Rock Mech. Min. Sci.*, **40**(5), 687-700.

Hoek, E. and Bieniawski, Z.T. (1965), "Brittle fracture propagation in rock under compression", *Int. J. Fracture*, (1), 137-155.

Itasca Consulting Group (2008), PFC^{2D} (Partical flow code in 2 dimensions) fish in PFC2D, Itasca Consulting Group; Minneaplis, USA, 20-22, 83-85.

Jing, L. and Stephansson, O. (2007), "Fundamentals of discrete element methods for rock engineering", *Theory and Applications*, Elsevier, Amsterdam, Netherlands.

Kusumi, H., Matsuoka, T., Ashida, Y. and Tatsumi, S. (2005), "Simulation analysis of shear behavior of rock joint by distinct element method", *Eurock 2005 — Impact of human activity on geological environment*, Taylor and Francis, London, UK, pp. 281-286

Pal, S., Kaynia, A.M., Bhasin, R.K. and Paul, D.K. (2012), "Earthquake stability analysis of rock slopes: A case study", *Rock Mech. Rock Eng.*, **45**(2), 205-215. DOI: 10.1007/s00603-011-0145-6

Park, J.W. and Song, J.J. (2009), "Numerical simulation of a direct shear test on a rock joint using a bonded-particle model", *Int. J. Rock Mech. Min. Sci.*, **46**, 1315-1328. DOI: 10.1016/j.ijrmms.2009.03.007

Park, J.W. and Song, J.J. (2013), "Numerical method for the determination of contact areas of a rock joint under normal and shear loads", *Int. J. Rock Mech. Min. Sci.*, 58,8-12. DOI: 10.1016/j.ijrmms.2012.10.001

Prudencio, M. and Jan, M.V. (2007), "Strength and failure modes of rock mass models with non-persistent joints", *Int. J. Rock Mech. Min. Sci.*, **44**(6), 890-902.

Pu, C.Z. and Cao, P. (2012), "Failure characteristics and its influencing factors of rock-like material with multi-fissures under uniaxial compression". *Trans. Nonferrous Met. Soc. China*, **22**, 185-191

Reik, G. and Zacas, M. (1978), "Strength and deformation characteristics of jointed media in true triaxial compression", *Int. J. Rock Mech. Min. Sci.*, **15**(6), 295-303.

Song, Y.L., Xia, C.C., Tang, Z.C. and Song, Y.J. (2013), "Numerical simulation and test validation for direct shear properties of rough joints under different contact states", *Chinese J. Rock Mech. Eng.*, **32**(10), 2028-2035, [In Chinese]

Sun, S.R., Sun, H.Y. and Wang, Y.J. (2014), "Effect of the combination characteristics of rock structural plane on the stability of a rock-mass slope", *Bull Eng. Geol. Environ.*, **73**(4), 987-995. DOI: 10.1007/s10064-014-0593-9

Wang, J., Li, S.C., Li, L.P., Zhu, W.S., Zhang, Q.Q. and Song, S.G. (2014), "Study on anchorage effect on Fractured Rock", *Steel Compos. Struct. Int.J.*, **17**(6), 791-801.

Yang, S.Q., Dai, Y.H., Han, L.J., He, Y.N. and Li, Y.S. (2009), "Uniaxial compression experimental research on deformation and failure properties of brittle marble specimen with pre-existing fissures", *Chinese J. Rock Mech. Eng.*, **28**(12), 2391-2404. [In Chinese]

Zhou, X.P., Bi, J. and Qian, Q.H. (2014), "Numerical simulation of crack growth and coalescence in rock-like materials containing multiple pre-existing flaws", *Rock Mech. Rock Eng.*, **48**(3), 1097-1114. DOI 10.1007/s00603-014-0627-4

CC